4-3-2014

The comparison of Signal Transducer and Activator of Transcription 3 to Green Fluorescent Protein as a marker for leptin receptor expressing neurons

Bhumit Desai

The comparison of Signal Transducer and Activator of Transcription 3 to Green Fluorescent Protein as a marker for leptin receptor expressing neurons

by

Bhumit Desai

Undergraduate honors thesis under the direction of

Dr. Neil Johannsen

Department of Kinesiology

Submitted to the LSU Honors College in partial fulfillment of the Upper Division Honors Program

April 3rd, 2014

Louisiana State University
& Agricultural and Mechanical College
Baton Rouge, Louisiana

Obesity – A Current Epidemic

The current state of obesity has prompted new nutritional and physical interventions attempting to treat the disease. Obesity's prevalence among global populations and costs of treatment have led researchers to view this growth as a serious epidemic. The threat as a risk factor for other diseases such as cardiovascular disease (CVD) and Type 2 Diabetes (T2D) increases the level of obesity's danger (Story, Neumark, Sherwood, & Holt, 2002). The fundamental concept behind obesity is that body fat increases when energy intake consistently exceeds energy expenditure (Block, Desalvo, & Fisher, 2003). Specific physiological characteristics along with genetics play a major influence on the prevalence of obesity (Story et al., 2002).

National health surveys conducted between 2007 and 2009 show that the prevalence of obesity in America was approximately 34.4% (Wimalawansa 2013). With such high levels among the population, recent epidemiologic studies have drawn connections to multiple comorbidities. The most common among these include T2D, CVD, metabolic syndrome, dyslipidemia, hypertension, and coronary artery disease (Story et al., 2002). According to the Nurses' Health Study data, the risk of diabetes is 50- to 60-fold higher when BMI is greater than 35 (Wimalawansa 2013).

Not only does obesity lead to adverse health effects, but also health care costs are significantly affected. The number of patients that require treatment are steadily increasing. Current costs attributable to treating obesity alone reached approximately US $78 billion in 2003, with costs escalating up to US $180 billion per year over the last decade (Wimalawansa 2013). Lowering excess weight in obese patients has major beneficial outcomes such as an improved quality of life and cost reductions.

Obesity consists of various pathological, inflammatory, and endocrine entities, including excess production of adipocyte-related hormones and cytokines. Prevailing data suggests that obesity is due mostly to the combination of two key factors: 1) unhealthy eating habits with high consumptions of calorie-dense diets, and 2) inadequate physical activity (Wimalawansa 2013). Fat accumulation, particularly visceral fat, plays a major role as a CVD risk for obesity patients (Block et al., 2002). The breakdown of lipids in adipose tissue leads to varying sensitivity towards insulin and epinephrine depending on adipocyte location (Wimalawansa 2013). Understanding the inner workings of adipose tissue regarding metabolism and energy expenditure has been adopted in clinical settings to effectively treat obesity.

Obesity has quickly become one of the biggest public health concerns in North America. New research methods focused on the role of adipose tissue in decreasing the total amount of visceral fat present can positively affect obesity treatment. The varying causes of obesity such as diet-induced, genetic, and infection have increased its prevalence. The following section delves deeper into details of adiposity-related obesity and its biochemical mechanisms.

Leptin

The hormone leptin is derived from adipose tissue. Leptin regulates feeding and energy expenditure in mammals. The hormone is produced in proportion to fat stores and is essential for processes such as reproduction, tissue remodeling, and growth (Münzberg & Myers, 2005). Adequate leptin levels lead to the repletion of body energy stores and thus suppress food intake and allow energy expenditure. Lack of leptin signaling due to

mutation of either leptin or the leptin receptor always attributes to increased food intake and reduced energy expenditure (Myers, Cowley, & Münzberg, 2008). Limited effects of leptin have been observed in obese individuals who display high circulating levels of leptin with no signs of weight loss – suggesting the idea of 'leptin resistance' (Münzberg & Myers, 2005).

Leptin acts via its receptor (LR), which is expressed in multiple sites of each cell. These leptin receptors exist in various isoforms – all of which are products of a single *Lepr* gene. They are divisible into three classes: secreted, short, and long. The secreted receptors are products of either alternatively spliced mRNA species or proteolytic cleavage products of membrane bound LR. The short and long forms contain exons 1-17 of the *Lepr* gene and therefore have identical extracellular and transmembrane domains (as well as the same first 29 intracellular amino acids). The difference between the two is their alternative splicing of 3' exons after the first 29 amino acids (Myers, Cowley, Münzberg, 2008). The long form of the leptin receptor, abbreviated as LRb, is the primary mediator of intracellular leptin signaling (Münzberg & Myers, 2005).

Moving to the specific circuitry controlled by leptin binding to the leptin receptor, two examples of neuron populations can be seen. The two populations in this signaling cascade are composed of three components. The first population synthesizes two components consisting of neuropeptide Y (NPY) and agouti-related peptide (AgRP), both of which play a role in appetite stimulation. The second population synthesizes pro-opiomelanocortin (POMC). Melanocortin receptors, melanocortin-3 and melanocortin-4, are G-protein coupled receptors that mediate effects caused by the neuron populations. NPY stimulates hunger directly due to its orexigenic (appetite stimulating) nature, while

AgRP stimulates hunger by inhibiting melanocortin receptor signaling (Myers, Münzberg, Leinninger, & Leshan, 2009). In neurons expressing POMC and LRb, POMC functions by producing α-melanocyte-stimulating hormone (α-MSH), which signals anorexia by signaling through activation of melanocortin receptors. LRb stimulates the production of POMC and thus the firing of these neurons. Leptin acts through LRb to suppress NPY/AgRP neurons. This is where leptin derives its capacity for regulation of appetite and energy expenditure (Münzberg & Myers, 2005). In summation, LRb signaling stimulates the production of anorexic neuropeptides and suppresses the action of orexigenic peptides as seen by experiments conducted in the best-characterized site of leptin action – the arcuate nucleus (ARC).

Mechanisms of Leptin:

LRb belongs to the interleukin (IL)-6 family of cytokine receptors, consisting of an extracellular ligand-binding domain, a single transmembrane domain, and a cytoplasmic signaling domain (White & Tartaglia, 1996).

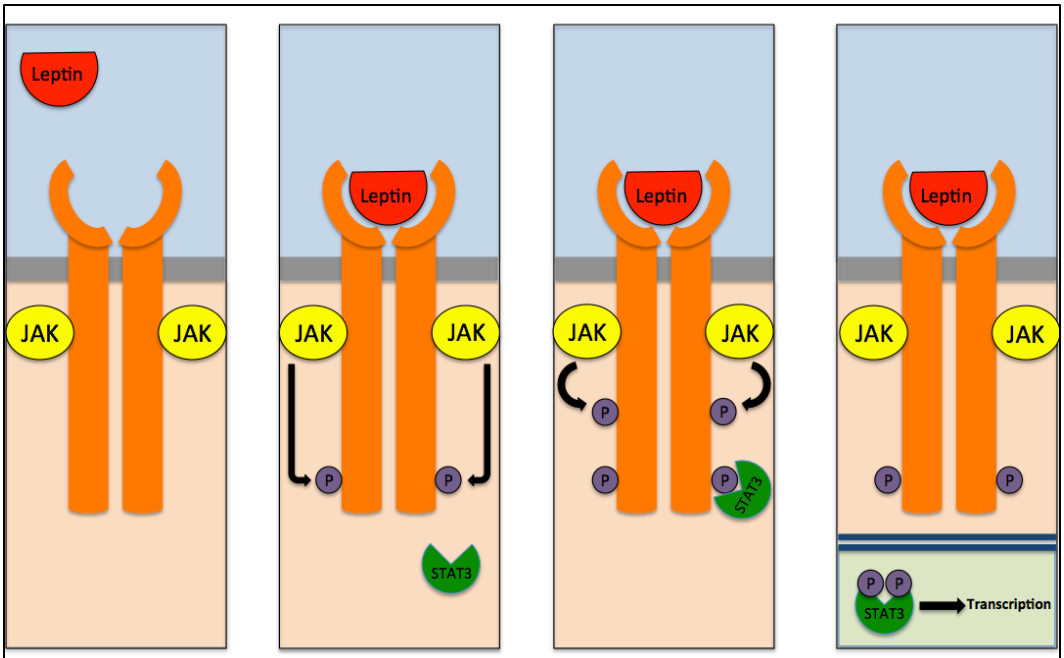

Fig. 1. The JAK-STAT Pathway. Leptin's chemical effect is transmitted from outside the cell through the membrane and into gene promoters on the DNA in the nucleus. This initiates DNA transcription in the cell. This specific system consists of the leptin receptor, Janus Kinase (JAK), and STAT3.

As shown above in Figure 1, the receptor signals via a non-covalently associated tyrosine kinase of the Jak kinase family (Taniguchi, 1995). Leptin binding alters the conformation of the LRb dimer, enabling transphosphorylation and activation of the intracellular LRb-associated Jak2 molecules (Couturier & Jockers, 2003). The activated Jak2 molecule then phosphorylates other tyrosine residues within the LRb/Jak2 complex to mediate downstream signaling (Banks, Davis, Bates, & Myers, 2000).

Three conserved tyrosine residues exist on the intracellular domain of LRb. They are Tyr_{985}, Tyr_{1077}, and Tyr_{1138} (White, Kuropatwinski, Devos, & Baumann, 1997). Tyr_{985} and Tyr_{1138} are phosphorylated when leptin binds. Tyr_{1077} is not phosphorylated by leptin binding and does not correspond with leptin signaling (Banks et al., 2000). Each pathway

also plays its own role in various processes, including transcription, activating protein signals, and activation of secondary pathways. The phosphorylation of Tyr_{985}, recruits the tyrosine phosphatase SHP-2. This pathway mediates the activation of p21ras (used as a signaling intermediary)→ extracellular-signal-regulated kinases (ERK) (intracellular signaling molecules involved in regulation of cell division function) signaling in LRb-expressing cells (Münzberg & Myers, 2005). Along with ERK stimulation, the LRb signal is attenuated through binding of the inhibitory molecule Suppressor of cytokine signaling 3 (SOCS3) (Bjorbaek, Lavery, Bates, Olsen, 2000). The second of the three LRb pathways, Try_{1077}, mediates the phosphorylation of Signal Transducer and Activator of Transcription 5 (STAT5) (Gong, Ishida-Takahashi, Villanueva, Fingar, 2007). STAT5 is used in cytosolic signaling and the mediation of expressing specific genes. However, its role in the regulation of physiology is not yet clear.

The third LRb pathway, and site of this research study's interest, involves the phosphorylation of Tyr_{1138}. This phosphorylation is the driving force behind Signal Transducer and Activator of Transcription 3 (STAT3) initiation during leptin action (Gong et al., 2007). Researchers previously demonstrated that LRb signals mediated by Tyr_{1138} are essential to the regulation of feeding and energy expenditure by leptin (Bates, Dundon, Seifert, Carlson, 2004; Bates, Stearns, Dundon, Schubert, 2003). STAT3 also serves as a feedback inhibitor for the SHP-2 domain-containing inhibitory signaling molecule SOCS3 (Bjorbaek, Elmquist, Frantz, Shoelson, 1998). Figure 2 (shown below) is a visual representation of the leptin → leptin receptor signaling cascade.

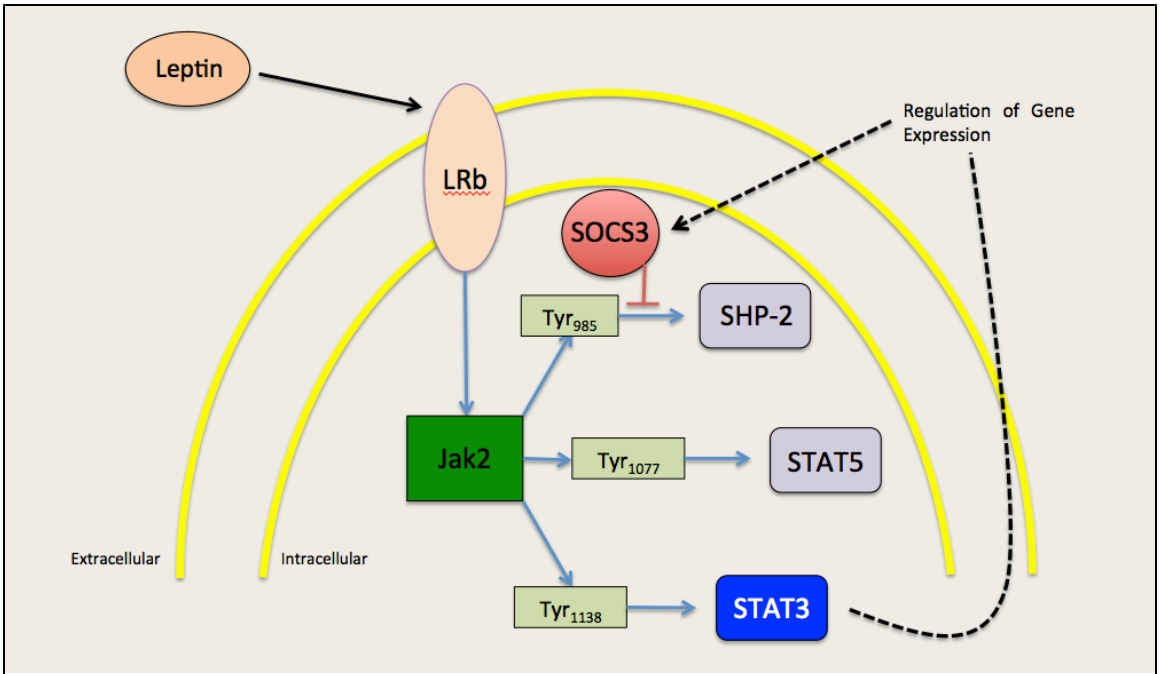

Fig. 2. This cartoon animation visualizes leptin action in the brain via the three tyrosine residues: Tyr_{985}, Tyr_{1077}, Tyr_{1138}. The intermediaries for each residue are also pictured. STAT3 levels (in blue) regulate the expression of SOCS3, an LRb inhibiting molecule. Leptin receptor activity is seen through the induction of phosphorylated STAT3 (pSTAT3) signals.

Lack of leptin signaling due to mutation of the leptin receptor or leptin itself is referred to as leptin deficiency (Münzberg and Myers, 2005). The result is an increase in food intake and reduced energy expenditure. Functional leptin receptors activate the JAK-STAT3 pathway resulting in the suppression of orexigenic neuropeptides and increase in anorexigenic neuropeptides (Morton, Cummings, Baskin, Barsh, 2006). In diet-induced obese rodents, the transport of leptin across the blood-brain barrier was observed to diminish even with fully functional leptin receptors (Morton et al., 2006). These lowered levels of leptin lead to profound effects in energy balance and hormone level. Some of the observed effects include overfeeding, suppressed energy expenditure, depressed reproductive hormones, and decrease in immune function (Ahima, Prabakaran, Mantzoros,

Qu, 1996). These observations demonstrate that the dominant role of leptin is to signal energy deficiency in the brain (Flier, 2009).

Previous studies suggest that the inhibitory feedback action of the LRb-SOCS3 pathway could explain the reduced effectiveness of increasing leptin concentrations in obesity. This phenomenon and physiologic conundrum is referred to as leptin resistance. One theory hypothesizes that at high levels of circulating leptin, increased baseline STAT3 would lead to increased SOCS3 production, which in turn would diminish the expected increase in LRb signaling (Münzberg & Myers, 2005). These data are consistent with the claim that the intracellular LRb signaling cascade is inhibited in some way.

These pathways are important to understand given the lack of an antibody that can stain directly for the leptin receptor. An antibody would directly stain and identify any leptin receptor proteins located in the cell membrane. For this reason, the receptor cannot be directly used to identify areas of leptin action and alternative secondary pathways must be utilized instead. Leptin action occurs in several areas, including the areas of focus in this study: the arcuate nucleus (ARC), ventral medial hypothalamus (VMH), and mPOA (medial preoptic area). Leptin action has also been observed in the periphery, as well as the brain stem. The majority of leptin action, however, occurs in the brain. In order to determine leptin receptor function, two secondary pathways are used to provide discrete signs of leptin action with high confidence. Leptin receptor function can be seen effectively through Green Fluorescent Protein (GFP) and phosphorylated Signal Transducer and Activator of Transcription 3 (pSTAT3) pathways. GFP, the reporter gene, serves as an efficient indicator for selectively marking leptin receptor function in transgenic *LRbEGFP* mice (Cone, Cowley, Butler, Fan, 2001). pSTAT3 on the other hand, does not indicate leptin receptor directly

and is also activated by additional stimuli such as immune responses. A previous study showed that STAT3 is an indicator of leptin action via a POMC promoter through its derived peptide α-MSH (Münzberg, Luo, Nillni, Hollenberg, 2003). These cell bodies were compared with cell bodies in control rats treated with only phosphate buffered saline (PBS) and with no leptin treatment. Cells positive for pSTAT3 were not seen in the control animals' sections, thus proving pSTAT3 to be a reliable indicator of leptin action in leptin-treated animals. Figure 3 below shows the pSTAT3 difference in induction for vehicle animals versus leptin-injected animals in various areas of the rat brain.

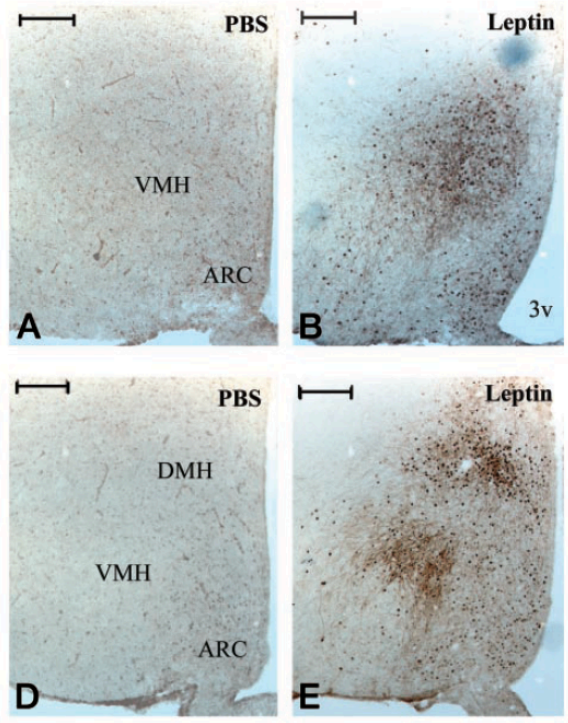

Fig. 3a. The image above shows activation of pSTAT3 phosphorylation in the mediobasal hypothalamus of vehicle rats treated with PBS (left column) verses rats injected with leptin (right column).
Münzberg et al., 2003

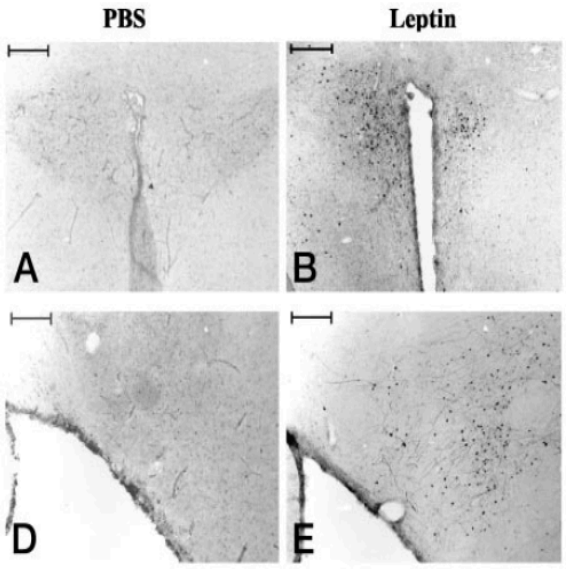

Fig. 3b. The image above shows activation of pSTAT3 phosphorylation in leptin treated animals (right column) vs. vehicle animals (left column) in the paraventricular nucleus (top row) and lateral hypothalamic area (bottom row).
Münzberg et al., 2003

Figure 3 has been adapted from the Münzberg et al. (2003) article in Endocrinology and has received the appropriate permissions to be used in this paper.

In order to solidify that pSTAT3 is a good marker for leptin action, positive signals are often co-expressed with those of GFP to further enhance confidence of the identity of leptin receptor neurons (Zhang et al., 2011).

pSTAT3 is the preferred indicator of leptin receptor neurons instead of pSTAT5 or SHP-2. There is little pSTAT3 in a normal, healthy animal, even though some baseline pSTAT3 signals are normal in the ARC. Deletion of leptin receptors resulted in the neuron-specific absence of leptin-induced pSTAT3, further indicating that leptin-induced pSTAT3 is a correlate of direct LRb function (Zhang et al., 2011). The primary goal of this study is to compare two well-established methods of detecting LRb in three hypothalamic sites in the mouse brain. The hypothesis predicts that the ARC will have the highest amount of induction for both leptin-induced pSTAT3 and LRb GFP neurons.

Cell Count Characterization

Materials and Methods

Animals. The protocols used to handle animals in this study meet the regulatory requirements of the Public Health Service Policy on Humane Care and Use of Laboratory Animals, the Animal Welfare Act and Regulations, and the Guide for the Care and Use of Laboratory Animals as per the Institutional Animal Care and Use Committee (IACUC). The animals were generously provided by Dr. Amanda Laque (Pennington Biomedical Research Center, Baton Rouge, Louisiana). The genotype of mice used for this study was a transgenic line derived from crossing *LRb^{cre}* and *RosaGFP*. The Cre double-homozygous genotype expresses an internal ribosomal entry site-driven second cistron that encodes cre-recombinase from the LRb-specific exon of the *Lepr* gene. GFP expression is dependent on the amount of Cre gene available. Excision of the stop codon in RosaGFP is required for GFP transcription, which leads to expression. Only two loxP sites exist in the entire gene where this excision can occur. The chances of perfect maximal GFP expression are therefore low, but are still sufficient for LRb neuron identification. In these *LLccgg* reporter mice, LRb-specific cre-recombinase was used to drive the cre-inducible expression of enhanced green fluorescent protein (EGFP). This specificity limits GFP expression to only LRb neurons (Zhang, Kerman, Laque, Nguyen, 2011).

Leptin-induced pSTAT3. The mice were first administered intraperitoneal leptin injections (1.25 mg/kg) 1 hour prior to perfusion. One-hour stimulation was chosen as a time where most LRb expressing sites show pSTAT3 induction.

Perfusion and histological processing. The mice were then deeply anesthetized with an overdose of pentobarbital (4 mg/kg) and perfused with saline followed by 10% Formalin via the left ventricle. During brain cutting, every 4^{th} section cut is placed in a respective well. This results in four series for each animal brain. Only one series of the brain was used for this study. This involves a less dense representation of brain sections. The reason for separating into four series is that one series sufficiently represents the brain areas studied. Additionally, the three extra series allow backups in case the experiment does not yield the expected results. Ruining an entire brain would require that the initial treatments be administered again. The extra animals needed to complete the experiment would be an undesirable approach. The aim should be to use the least amount of animals possible to complete the experiment. A successful experiment could then allow further research on the brain under the same treatment using the other series. The prepared brain series was then stored for free-floating immunohistochemistry to detect the signal.

Immunohistochemistry Analysis. Immunohistochemistry (IHC) is a technique used to detect antigens/proteins in tissue sections through specific antibody-antigen reactions. These antibody-antigen reactions are visualized with the use of a conjugated enzyme or fluorophore DyLight 488. Enzymatic-mediated detection of antibody-antigen reactions may also be amplified using biotin- avidin/streptavidin complex (ABC) kits. When biotinylated antibodies are used, an avidin/streptavidin complex consisting of multiple horse-radish peroxidase (HRP) can be bound, thereby increasing the number of localized enzymes per biotinylated antibody. Once antibodies and ABCs are bound, hydrogen peroxide (H_2O_2; HRP

substrate) is added along with an oxygen (O_2) sensitive chromogen, specifically 3,3'-diaminobenzidine (DAB). When H_2O_2 reacts with HRP O_2 is released, DAB is oxidized, becomes water insoluble, and is deposited locally as a dark brown precipitate. This precipitate is then visualized as a positive staining signal with bright-field microscopy. IHC stains are particularly useful for detecting visually unclear proteins such as pSTAT3.

The staining protocol began with a set of tissue samples fixed with formalin. Fixing the tissues prevents protein degradation while maintaining stability of the tissues for recognition of anatomical structures. The tissues were washed multiple times using phosphate buffered saline (PBS), which remove any unwanted solutions or particles left on the tissue. The next step quenched endogenous peroxidase activity in the tissues using an H_2O_2 solution in methanol. Next, the sections were treated with glycine, stopping any remaining fixative in the tissue. Following glycine treatment, sections were permeabilized with sodium dodecyl sulfide (SDS) to help antibodies penetrate the tissue and react with the antigens. The tissue sections were then blocked with normal donkey serum (NDS). This serum solution consists of an excess of free protein that fills up empty binding sites to minimize background signals that would arise from non-specific antibody binding. The primary antibody, Rabbit-α-pSTAT3 (Cell Signaling Technology), was then added to the tissue section in PBS solution at a 1:500 dilution ratio. The primary antibody distinguishes the type of signal that will be amplified by showing specificity for a single epitope. The tissues then incubated in primary antibody for 48 hours to ensure proper binding. After that sections were incubated in secondary antibody. The secondary antibody is always raised against the host species of the primary antibody. This guarantees binding of the secondary antibody to the primary, which will eventually bind the fluorophore. In order to

prepare for this secondary antibody the tissues again were washed with PBS to remove any excess unwanted primary antibody. Following the washes, the tissues were incubated in the secondary rabbit antibody, Donkey-α-rabbit-biotin (Abcam), for two hours in PBS solution at a 1:200 dilution ratio. Once the leptin-binding site was located, the signal was amplified using an avidin-biotin complex. The amplification is important for enhancing the resolution of the staining signal. The tissues were then exposed to H_2O_2 in the presence of DAB to develop the staining signal. These primary and secondary antibodies visualized pSTAT3 signals in the treated brain sections. The next step prepared the sections for GFP-induced leptin receptor neurons. The primary antibody used was Donkey-α-GFP (Abcam) at an incubation period of 48 hours in PBS solution at a 1:1000 dilution ratio. After several washes of PBS, the sections were treated with the GFP secondary antibody, Donkey-α-chicken-A488 (Invitrogen), for 2 hours in PBS solution at a 1:200 dilution ratio. After several more washes in PBS solution, sections were mounted onto slides and cover slipped before imaging.

Imaging and Estimate of Cell Counts. Three distinct areas of the brain were analyzed and counted after immunohistochemistry – the arcuate nucleus (ARC), ventral medial hypothalamus (VMH), and medial preoptic area (mPOA). The ARC can be seen with the formation of the median eminence at the inferior end of the brain (Bregma -1.22 mm). The arcuate nucleus continues well after the DMH has disappeared and the third ventricle has transitioned into the mammillary recess (Bregma -2.80 mm). The VMH is more caudal bordering the third ventricle after the DMH has disappeared, where the arcuate nucleus becomes prominent (Bregma -1.34 mm). The rostral sections just prior to the formation of

the third ventricle characterize the mPOA (Bregma 0.26 mm). The mPOA then moves upward and out with the progression of the ventricle up until the appearance of the optic tract (Bregma -0.58 mm). From most rostral to caudal the order of areas is as follows: mPOA, VMH, ARC. In order to numerically identify each of these specific areas, bregma is often used in stereotaxic surgery as a starting point of reference. Bregma refers to the anatomical point on the skull at which the coronal suture is intersected perpendicularly by the sagittal suture. All bregma markings for the sections used in this study are derived from the Mouse Brain atlas written by Paxinos and Franklin (2004). A prominent image of each location can be seen in Figure 4 below. Figure 4 shows a sagittal view of each respective area of focus in the mouse brain after GFP staining. These images show a rostral to caudal extension of GFP signaling. The mPOA starts at the rostral end and the ARC represents the caudal end of the brain.

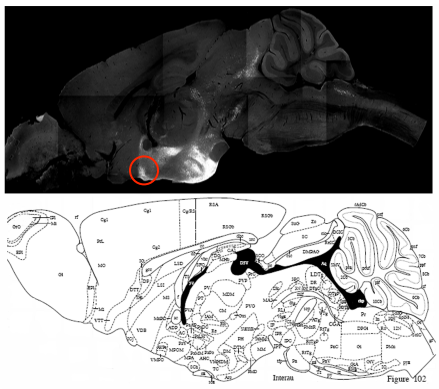

Fig. 4a. A sagittal view of the neuroanatomical location of LRb neurons in the mPOA visualized with GFP.

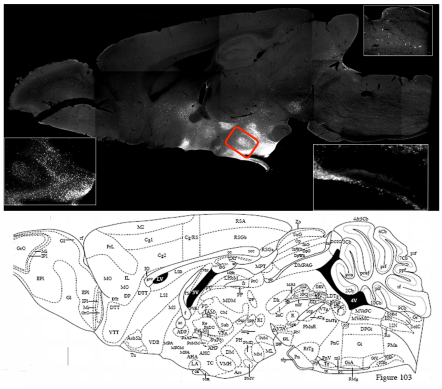

Fig. 4b. A sagittal view of the neuroanatomical location of LRb neurons in the VMH visualized with GFP.

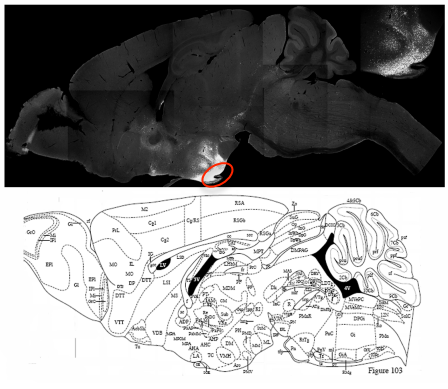

Fig. 4c. A sagittal view of the neuroanatomical location of LRb neurons in the ARC visualized with GFP.

The IHC staining was visualized using a fluorescent microscope (Olympus BX51), and images were taken with a digital camera (Olympus DP30BW). pSTAT3 signals are visualized using a bright field microscope. The fluorophore GFP is visualized with a mercury light source (Olympus). Using a filter allows proper excitation and emission of GFP at a 488 nm emission wavelength. Identical images were taken for double IHC (one with bright field, one using the green filter Alexa-488 filter), overlaid, and pseudocolored using Olympus Software and Adobe Photoshop (Adobe Systems). A red overlay was used to visualize pSTAT3 induction and a green overlay was used to visualize GFP neurons. Figure 5 shows coronal views of visualized pSTAT3 and GFP signals overlaid to complete colocalized and individual cell counts. These images show a higher magnification along with colocalization compared to the sagittal view sections in Figure 4.

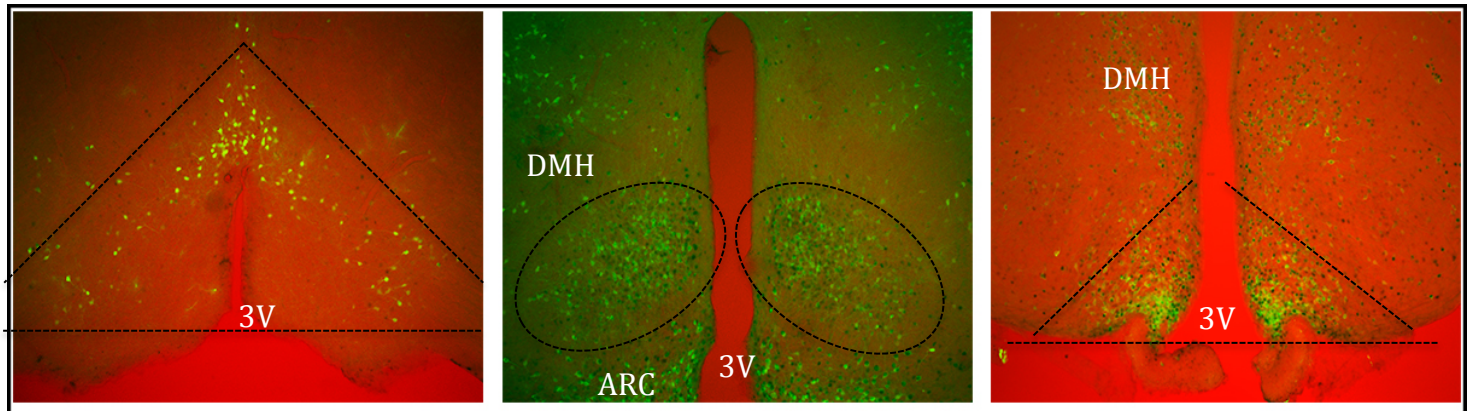

Fig. 5a. **Fig. 5b.** **Fig. 5c.**

Overlaid sections of the mPOA (a), VMH (b), and ARC (c) showing both GFP and pSTAT3 staining in a coronal view. The areas of focus are outlined by the dotted lines.

The reasoning behind the overlay is that the green correlates to green-fluorescence, while red contrasts well and makes neuron differentiation easier when counting cells. Contrast and brightness were adjusted for fluorescent signals with Adobe Photoshop (Adobe Systems) for better visualization of neurons. While all cells were edited to enhance visualization of neuron populations, steps taken to ensure the images remained comparable. First, all pictures were taken using the same exposure time across all sections for each respective magnification. In order to maximize cell body visual identification, GFP images were modified by setting exposure time as low as possible. This visualized fluorescent induction signals against a dark background as best as possible. pSTAT3 images on the other hand, had higher exposure times to better visualize dark cell bodies against a bright background. After overlays, each image was edited in Photoshop using the same process. An initial level was set for the Red channel to enhance pSTAT3 induction. This level setting was saved as a preset and used for the remainder of the image enhancements. Lastly, each image was adjusted using Contrast/Brightness in Photoshop. The same numbers were used across all images to maintain uniformity of protocol. This ensured the images were comparable across all sections of every brain. The universal image enhancements also account for differences in induction intensity. Brighter signals entail neurons embedded closer to the outer edge of the brain tissue, whereas dark or unclear signals suggest cell bodies deeply embedded in the tissue. Estimates of cell counts were taken to quantify the number of leptin-induced pSTAT3 neurons colocalized with *LRbEGFP*, as well as total *LRbEGFP* cells. The first step after capturing the images was to section off the areas of interest (mPOA, VMH, ARC) in each respective brain section. A total of three animals were analyzed for this study, with one series of sections used for each brain, as

previously mentioned. For each area of the brain, three sections were used that correlated to a specific area. The sections were identified and analyzed in a rostral to caudal order. This offered multiple angles of all the possible leptin-induced signals for each area of investigation. The areas were identified using two important sources. The first was a mouse atlas assembled in a previous study showing ideal GFP induction in leptin treated mice. This confirmed what the GFP induction images should look like in terms of signal intensity and neuroanatomical locations of induction. The second source included talks with Dr. Heike Münzberg at Pennington Biomedical Research Center based on her knowledge and experience working with mouse models for a number of years. Her expertise was paired with the published drawings from the mouse atlas (Paxinos & Franklin, 2004) to confirm the areas' correct location. Once each area was identified, the neuron cell bodies were sectioned off based on population density. This was accomplished by finding the cell bodies that fell inside of a geometric shape of the entire population. The shape tool in Photoshop was used to draw ovals around each VMH population, and triangles for each ARC and mPOA population. Cell bodies falling outside of these shape ranges were not included in cell count estimations. Once the areas were identified and sectioned off, the next step was to count the viable induction signals. Photoshop's Count Tool feature was used for all cell counts to guarantee specific cells within the areas of interest were not counted twice. For GFP counts, all cell bodies were counted that displayed a clear ovular shape with a nucleus inside. For many arbitrary signals where the outside shape of the cell body was not completely visible, the cell was counted if the nucleus along with a round outer edge was seen. For pSTAT3 counts, an induction signal consisted of a completely black, round cell body. Careful consideration was taken to ensure

all counts made were of cell bodies and not of background noise or imperfections in the tissue. The third type of cell count, colocalized cells, consisted of a pSTAT3 signal embedded within a GFP signal. GFP signals were consistently larger than pSTAT3 signals, meaning that pSTAT3 was engulfed by each GFP-induced cell body. Colocalized cells were counted as cells that showed this engulfed pairing. In order to double check that colocalized cells were not counted twice or unidentified previously, the counts from pSTAT3 and GFP were overlaid. Count markers for pSTAT3 and GFP that overlapped were counted as colocalized cells. The colocalized marker was then confirmed by checking to see if the pSTAT3 signal was engulfed by a GFP signal.

Once all cell counts were carried out for one brain section, GFP, pSTAT3, and colocalized numbers were recorded in a Microsoft Excel spreadsheet to be used later for data analysis. This procedure was then repeated for three tissue sections of all three areas for all three test animals.

Results

In this cell count characterization study, a population of LRb neurons was outlined in the mPOA, VMH, and ARC. To clarify the anatomical location of each of these areas, the mouse brain atlas was used (Paxinos & Franklin, 2004). The goal was to compare two methods of visualizing leptin receptor expression neurons and outline advantages and disadvantages for each. The results differed depending on which method was used – either identifying LRb through GFP neurons or noting the leptin-induced pSTAT3 signals. The absolute differences were represented by a ratio of pSTAT3 induction to GFP neurons. The higher the ratio is to 1, the higher degree of overlap between both methods for visualizing LRb expression. A second method also exists for testing the confidence of pSTAT3 induction. The percentage of colocalized cells out of total pSTAT3 induction can determine pSTAT3's competency as an indicator of LRb presence. The data will be represented in two discrete forms. The comparison between total GFP and total pSTAT3 will be stated through cell count numbers. The colocalization method will then be shown through two types of graphs. The first will show the total absolute number of pSTAT3 signals vs. colocalized GFP signals to show the amount of induction. The second graph will show the amount of GFP signals colocalized in total pSTAT3 signals in order to clearly visualize percentages. Each of the three areas will now be focused on individually.

Medial Preoptic Area (mPOA). In the mPOA, the amount of total GFP neurons was counted in 3 sections identified as part of the mPOA in all three animals. The total count was 416 neurons. The mean value of total GFP in each animal (including 3 sections per animal) was 139 neurons. The total amount of pSTAT3 induction noted in all three sections of the mPOA for each animal was counted at 368. The mean value of total pSTAT3 in each animal was 123. This leads to a ratio of 368:416 or 0.88:1 or 88%. This states that 88% of the neurons identified by GFP staining for LRb were also identified by pSTAT3 induction.

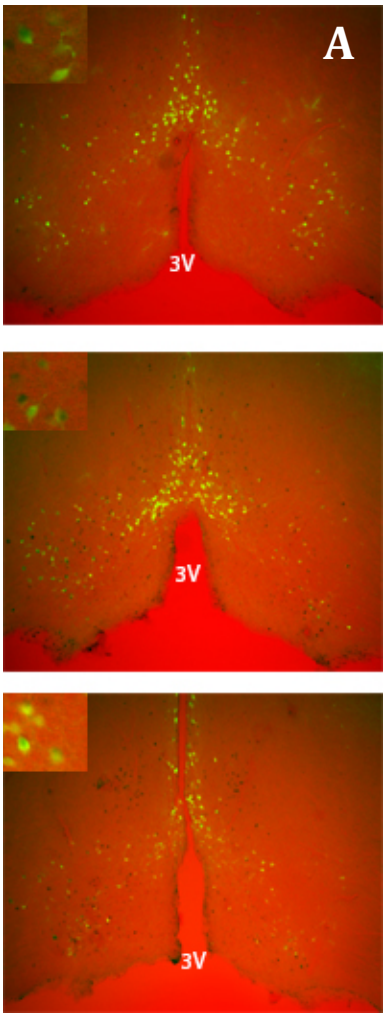

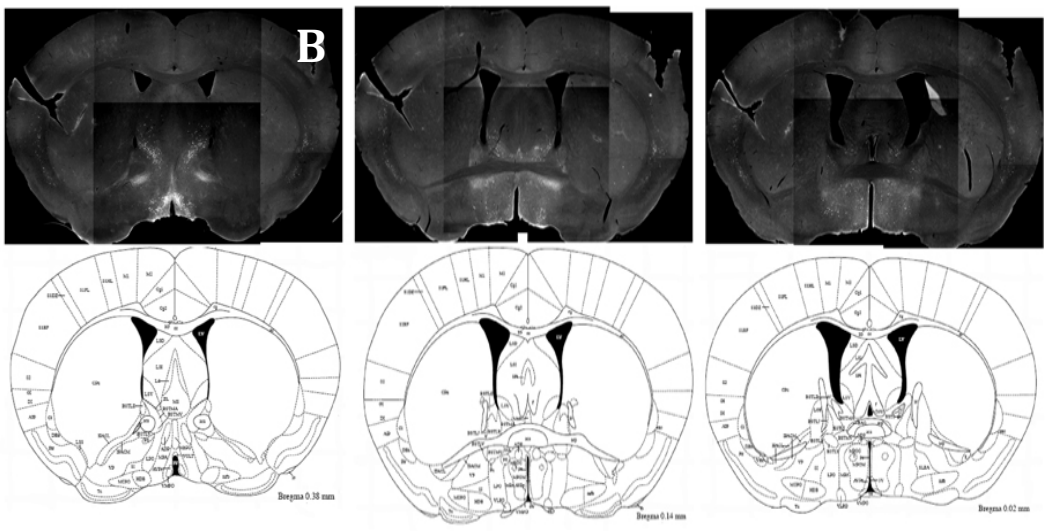

Bregma 0.38 mm Bregma 0.14 mm Bregma 0.02 mm

Fig. 7. Coronal sections of the mPOA. 7A shows colocalized sections of both pSTAT3 induction and GFP expression moving rostral to caudal used in this experiment. 7B shows a lower magnification of only GFP neurons in the mPOA characterizing the expected sites of leptin action (rostral to caudal) from a previous experiment.

Figure 7 shows the colocalized sections used in this experiment for mPOA cell counts. The three images in 7A were used for both colocalized counts and individual pSTAT3 and GFP signal populations. 7B outlines the expected GFP expression in the mPOA under a lower magnification.

In the second method, only 38% of total pSTAT3 induction signals were colocalized with GFP neurons. This method takes the potential location of LRb neurons and provides more detailed information about each signaling molecule. The fact that only 38% of neurons were colocalized says that out of the total number of signals given off by pSTAT3, only 38% of them were being in the same exact spot GFP indicated as being a potential axon pathway location for a LRb neuron. This gives two possible conclusions; the first being that 62% of pSTAT3 induction signals were caused by another stimulus, or second that GFP is not an accurate marker of LRb neuron populations.

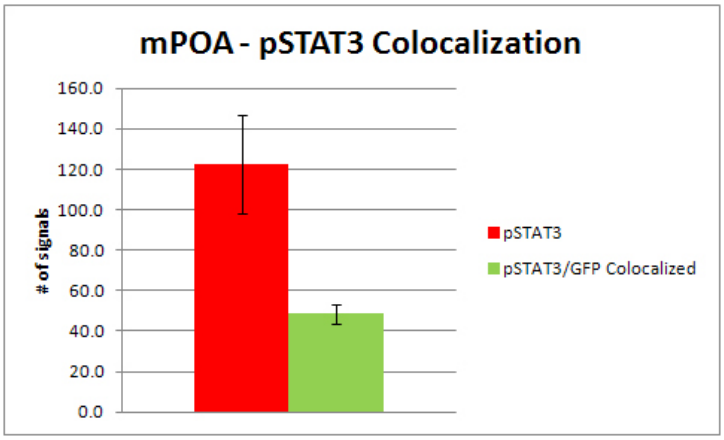

Fig. 8A. The graph shows the total amount of pSTAT3 induction compared to how many of these signals colocalized with GFP neurons in the mPOA.

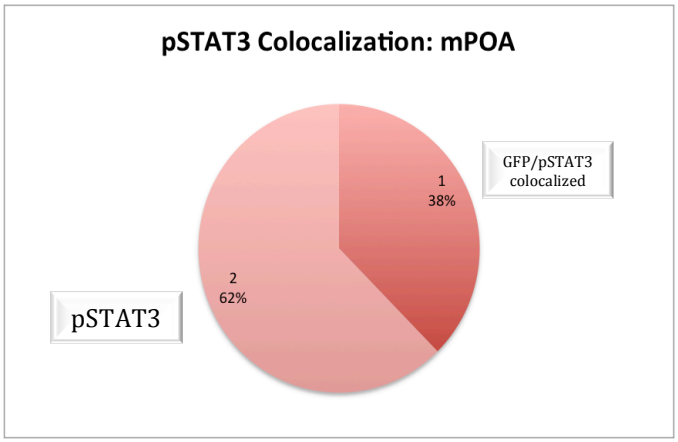

Fig. 8B. The pie chart represents the percentage of GFP neurons colocalized with the total number of pSTAT3 induction.

Figure 8 shows the graphical data for colocalization cell counts. The bar graph represents the absolute number of total pSTAT3 versus colocalized GFP/pSTAT3. The pie chart represents the same data as a percentage.

Ventral Medial Hypothalamus (VMH). In the VMH, the amount of total GFP neurons were also counted in 3 sections for all three animals. The total count was 2,280 neurons. The mean value of total GFP in each animal (including 3 sections per animal) was 760 neurons. Note the sudden increase in number of neurons from the mPOA to the VMH. The total amount of pSTAT3 induction noted in all three sections of the VMH for each animal was counted at 2,743. The mean value of total pSTAT3 in each animal was 914. This leads to a ratio of 2743:2280 or 1.2:1 or 120%. This indicates more potential LRb neurons were identified by pSTAT3 induction than by GFP staining in the VMH counts.

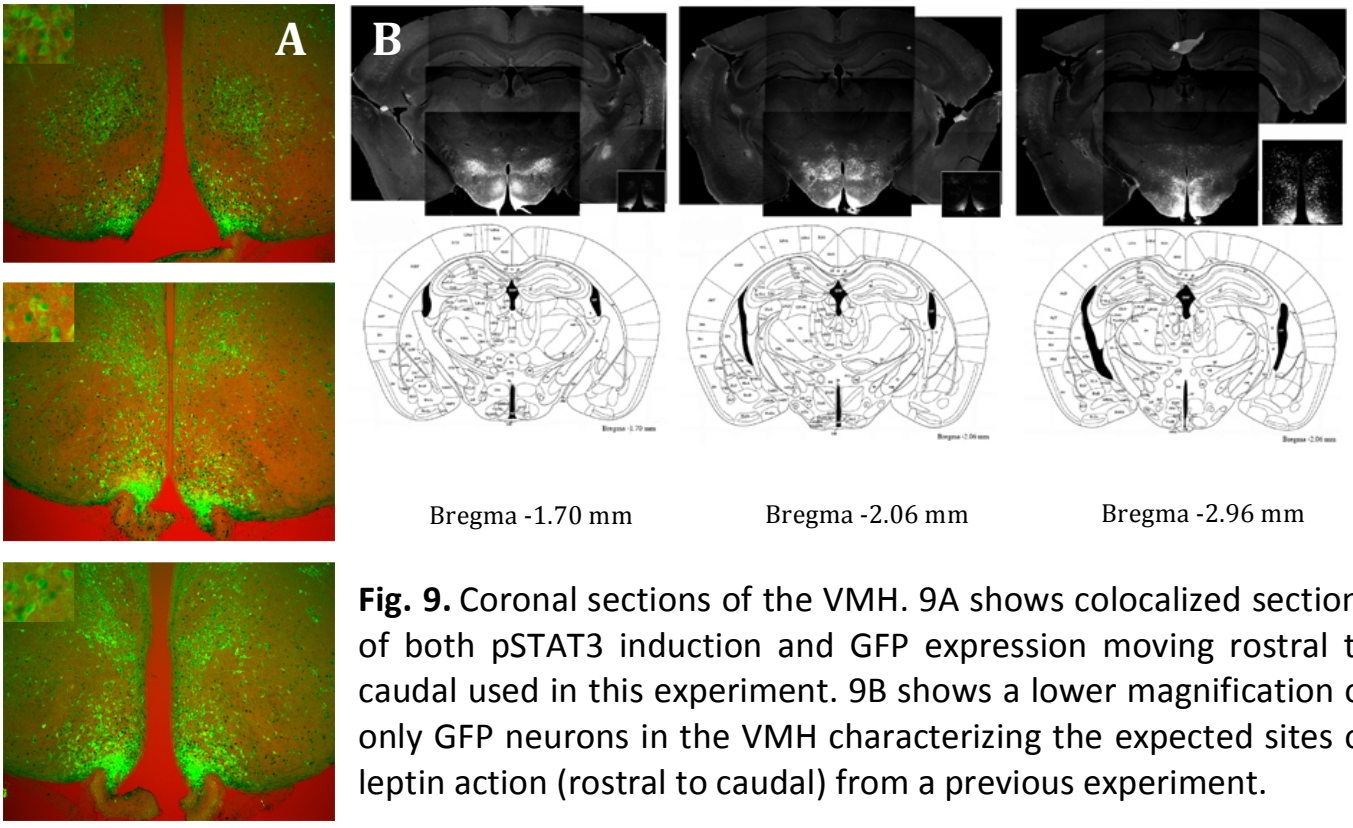

Fig. 9. Coronal sections of the VMH. 9A shows colocalized sections of both pSTAT3 induction and GFP expression moving rostral to caudal used in this experiment. 9B shows a lower magnification of only GFP neurons in the VMH characterizing the expected sites of leptin action (rostral to caudal) from a previous experiment.

Figure 9 shows the colocalized sections used in this experiment for VMH cell counts. The three images in 9A were used for both colocalized counts and individual pSTAT3 and GFP signal populations. 9B outlines the expected GFP expression in the VMH under a lower magnification.

Using the second method of comparing pSTAT3 to GFP for presence of LRb neurons, 57% of total pSTAT3 induction signals were colocalized with GFP neurons. The VMH showed a markedly higher percentage of colocalization compared to the mPOA. 57% of pSTAT3 induction correctly approximated the axon pathway location for a LRb neuron. While 57% is higher than rates seen in the mPOA, a high vote of confidence does not exist.

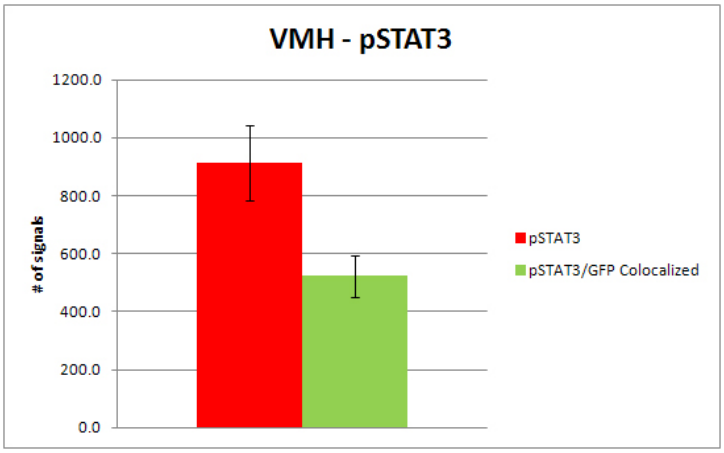

Fig. 10A. The graph shows the total amount of pSTAT3 induction compared to how many of these signals colocalized with GFP neurons in the VMH.

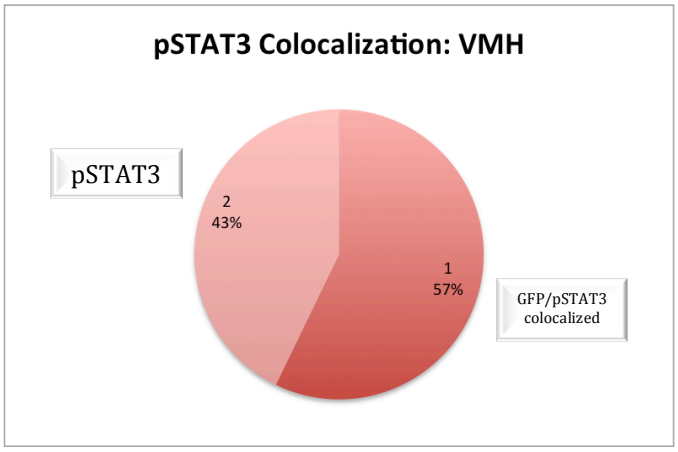

Fig. 10B. The pie chart represents the percentage of GFP neurons colocalized with the total number of pSTAT3 induction.

Figure 10 shows the graphical data for colocalization cell counts. The bar graph represents the absolute number of total pSTAT3 versus colocalized GFP/pSTAT3. The pie chart represents the same data as a percentage.

Arcuate nucleus (ARC). The arcuate nucleus extends extensively through the brain, but for uniformity across all three animals, only the three sections shown were used for cell counts. These three sections are representative of the arcuate nucleus neuron population for this study since this specific range was identified and counted across three animals. In the ARC, the amount of total GFP neurons was counted in 3 sections across all three animals. The total count was 1,384 neurons. The mean value of total GFP in each animal was 461 neurons. Although the ARC has been proven to be the most well known area of leptin action, the strict borders placed around the ARC during cell counts (in order to maximize colocalization percentages) may account for the decrease in neurons compared to the VMH. The total amount of pSTAT3 induction noted in all three sections of the ARC for each animal was counted at 1,472. The mean value of total pSTAT3 in each animal was noted to be 491. This leads to a ratio of 1472:1384 or 1.06:1 or 106% of the amount of GFP neurons. This ratio indicates that pSTAT3 induction was higher in the ARC than GFP neuron excitation.

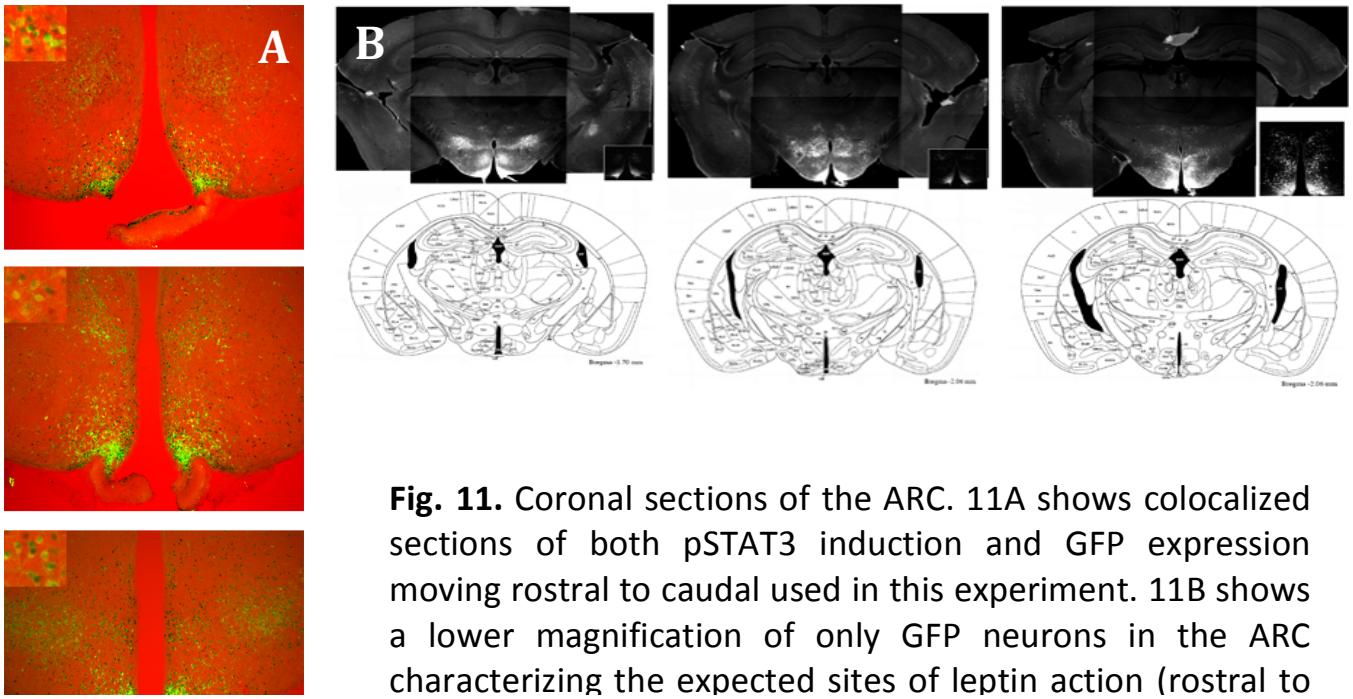

Fig. 11. Coronal sections of the ARC. 11A shows colocalized sections of both pSTAT3 induction and GFP expression moving rostral to caudal used in this experiment. 11B shows a lower magnification of only GFP neurons in the ARC characterizing the expected sites of leptin action (rostral to

Figure 11 shows the colocalized sections used in this experiment for ARC cell counts. The three images in 11A were used for both colocalized counts and individual pSTAT3 and GFP signal populations. 11B outlines the expected GFP expression in the ARC under a lower magnification.

In the second method of analysis of pSTAT3 and GFP for presence of LRb neurons, 84% of total pSTAT3 induction signals were colocalized with GFP neurons. Finally, the ARC shows a remarkably high percentage of colocalization that can be counted on to approximate for presence of LRb neurons. 84% of pSTAT3 induction correctly approximated the axon pathway location for a LRb neuron indicated by GFP excitation. This high confidence was consistent with previous knowledge that the ARC is the highest brain center of leptin action as well as the most studied.

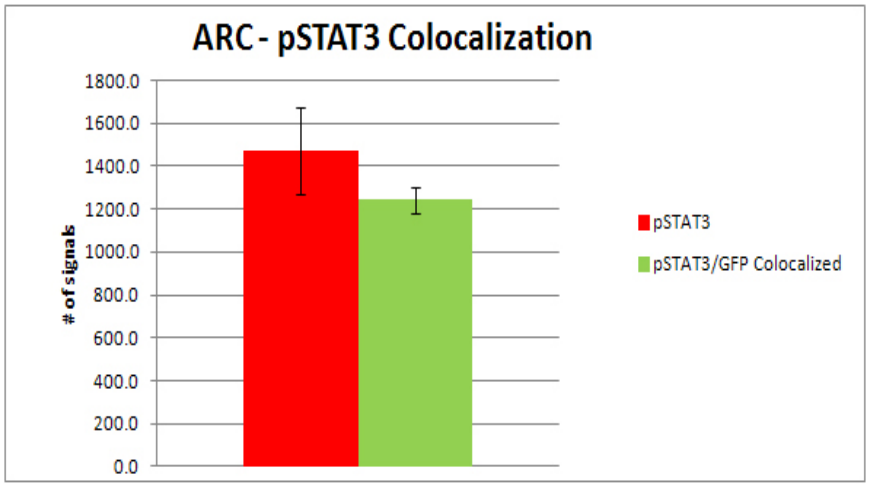

Fig. 12A. The graph shows the total amount of pSTAT3 induction compared to how many of these signals colocalized with GFP neurons in the ARC.

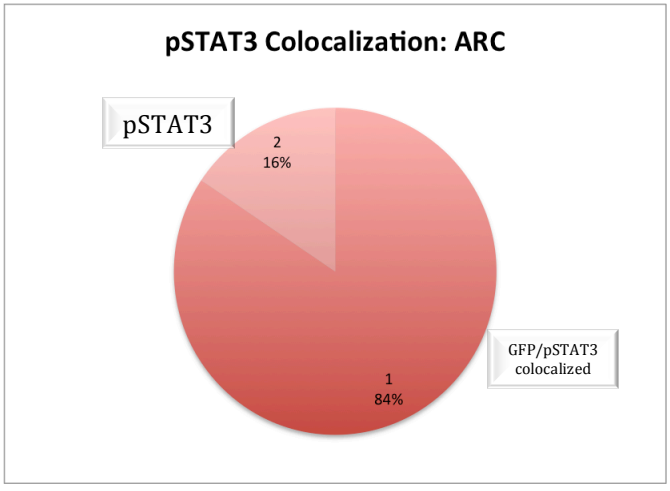

Fig. 12B. The pie chart represents the percentage of GFP neurons colocalized with the total number of pSTAT3 induction.

Figure 12 shows the graphical data for colocalization cell counts. The bar graph represents the absolute number of total pSTAT3 versus colocalized GFP/pSTAT3. The pie chart represents the same data as a percentage.

Discussion:

A wide array of results was observed in the 3 areas of focus for this study. The mPOA did not show a high colocalization of pSTAT3/GFP, however a fair amount of pSTAT3 induction was still seen. The conclusion may be drawn here that pSTAT3 induction was less than the number of signals comparative to the other two sections. One of the limitations of pSTAT3 is its activation by other stimuli. The results of this study however, were not limited by other secondary stimulation. Looking at the absolute cell count numbers of total GFP vs. total pSTAT3, the number of both pSTAT3 and GFP neurons compared to the VMH and ARC suggest less leptin action takes place in the mPOA. However, a low amount of signaling does not necessarily mean unimportant signaling. Leptin receptor activation in the mPOA may very well play a major role in energy expenditure and metabolism.

The VMH showed a moderately higher colocalization percentage than the mPOA at 57%. Therefore, the VMH has more leptin action than the mPOA. However, the colocalization percentage is not high enough to say with confidence that the pSTAT3 signals are all indicative of LRb neurons. Percentages under 70% do not provide high enough confidence about the pSTAT3 signals' role as indicators of LRb neurons.

The ARC gave the best results out of the three areas focused on in this study. Not only was the colocalization percentage high, but also the ratio of GFP neurons to pSTAT3 signals was very close to 1. A commonly used benchmark to evaluate the confidence of results is cut off at 70% and above. The colocalization seen in the ARC was well over 70%, which informs with high confidence that the pSTAT3 induction seen is indicative of LRb

neuron populations. An equal representation between GFP and pSTAT3 is also valuable because that's what the entire goal of the study encompasses – to visualize leptin action through the identification of LRb neurons using these signaling molecules. Another trend noticed was an increase in pSTAT3/GFP colocalization as observations moved from rostral to caudal in the mouse brain. This may suggest that leptin has more of an effect in the caudal areas of the brain. The data also supports this hypothesis, as total neuron cell body numbers increased from rostral to caudal.

pSTAT3 compared well with GFP for the absolute number of neurons stimulated, but this does not provide much information about identifying LRb neuron populations. Simply a general scope is offered to compare pSTAT3 signals to GFP neurons. A ratio of 1 or above is favored because everything GFP identified as a potential LRb neuron was also identified by pSTAT3. A very high colocalization also implies that both methods identified the same exact neurons as potential LRb neuron populations. However, when viewing colocalization percentages pSTAT3 did not correlate well to GFP in two of the three sections of focus. This indicates that pSTAT3 and GFP are both competent identifiers of leptin receptor function, but do not consistently visualize the same neuron populations across all brain tissues.

Leptin action and identification of LRb function have been well studied in the VMH, as well as the ARC. The mPOA does not have much information out currently, making the area a prime candidate for this study. The data suggested that the mPOA has relatively fewer signs of leptin action via both GFP signals and leptin-induced pSTAT3. From this data one may conclude that the mPOA could in fact be a major player for obesity treatment with further studies about specific neuron populations.

Harveen Dhillon and team recently conducted a study documenting the VMH. The ARC was first emphasized as an especially important part of leptin action. However, other sites of leptin action are also activated through LRb neurons. The research team made this conclusion by using Cre-lox conditional gene-knockout technology to delete the leptin receptors only correlated to POMC (ARC-specific) neurons, which resulted in mild obesity. These animals were then compared to animals that had POMC leptin receptors deleted elsewhere in the brain, which led to massive obesity. The monumental difference in obesity lends to the notion that areas other than just the ARC are involved in leptin's anti-obesity effects (Dhillon et al., 2006). They then tested their hypothesis about the VMH's effects on leptin action's role in energy expenditure by generating mice lacking leptin receptors exclusively on SF1 neurons (found only in the VMH). The results of the VMH study suggested that SF1 neurons in the VMH are directly activated by leptin, seen through comparisons to SF1 neurons without leptin receptors that did not activate (Dhillon et al., 2006). Additional tests also showed that deletion of SF1 neurons led to abnormal VMH development that led to obesity (Dhillon et al., 2006). Comparing the results of the VMH study to the current findings, the results agree that the VMH has an important role in controlling body weight. In fact, the VMH showed the largest number of GFP neurons as well as pSTAT3 induction, suggesting that leptin action is incredibly strong in this area.

The third area of focus in this study, the arcuate nucleus, has been well studied concerning the effects of AgRP and POMC neurons. A study conducted by Jennifer Hill and team in 2008 used PI3K, a signal transducer enzyme mediated through the Jak2 signaling pathway, to test leptin's effect on POMC neurons. Their study inhibited PI3K activity to test if changes were seen in depolarization rates, which would support POMC's effect on leptin

action mechanism. Mice with genetically disrupted PI3K signaling in POMC cells failed to have increased firing rates in response to leptin, which allowed them to conclude that PI3K signaling in POMC neurons is essential for leptin-induced activation (Hill et al., 2008). The Hill study of POMC neurons provided support for the arcuate nucleus' role in LRb function and leptin action. The data from the current study also supports the ARC's role in leptin-induced pSTAT3. An 84% colocalization of pSTAT3 with GFP neurons provides great confidence for the presence of LRb neuron populations in the ARC. Connecting these results with information presented in the introduction, many of the LRb neuron populations identified may be the pathways responsible for AgRP and POMC activation in these animals.

While pSTAT3 is typically a good indicator of LRb signaling, one of the main weaknesses of this method is the induction by other stimuli. Immune responses to interleukins and cytokines stemming have been known to cause induction of pSTAT3. The animal's physiologic response to infection would induce STAT3 signaling. Paired with the fact that leptin-induced pSTAT3 also includes the difficulty of an indeterminate maximum amount of signals, the number of actual leptin receptor neurons is often overestimated. This can lead to pSTAT3 errors, indicating LRb neurons where none actually exist. Another weakness includes the early development of animals and the timing of these signaling pathways. For example, even if leptin may initially activate pSTAT3 induction, an uncertainty exists if all of the signals seen are as a direct result of leptin action or secondary stimuli. The pathway follows that leptin first binds the leptin receptor, activates pSTAT3 in the nucleus, then the axonal projections then have an effect on a secondary neuron. The neurotransmitters released here activate pSTAT3 effects in the body. Based on this

proposed pathway, when no functional leptin receptors are present, pSTAT3 induction is still seen. One of the hypothesized reasons could be a difference in the timing of injecting leptin. The earlier that leptin is injected, the more time that is available for the necessary antibodies to bind, and thus lead to the proper signal induction. Along these lines, a clear weakness is also seen for GFP expression. GFP expression is dependent upon the amount of Cre-LoxPGFP available. Every cell in the body already exhibits a nucleus containing a floxed GFP gene (meaning a DNA sequence encoding for GFP sandwiched between two lox P sites). A lox P site refers to a specific 34-basepair sequence on the genome. Once a gene has been floxed, a sequence can be deleted, translocated, or inverted using Cre-lox recombination. The GFP (end-product) can only be transcribed if the stop sequence is cut out from this gene. For every single cell, Cre must be expressed in the cell, transported to the nucleus, and identify the correct area of the genome (which contains only two sites where Cre can cut). Cre must find at least one of those sites in order to function properly (finding both is ideal). The more Cre available in the nucleus, the more likely that the loxP sites will be found, bound properly, cut, and properly reconnected. If all these actions follow one another chronologically, only then can GFP be expressed. Another observation states that the less Cre available in the nucleus, the less likely GFP is expressed, and in turn the less chances that the neuron is excited. This is a caveat, because even though a leptin receptor neuron may be present, no stimulation will occur due to the lack of GFP expression. GFP expression must also be high enough to overcome the stimulation threshold. Once all the proper sequences have been excised and ligated, GFP starts to be transcribed. When little is GFP present, the minimum threshold will not be reached, and antibodies will not bind for fluorescent signaling. If an animal has just recently been

perfused and sacrificed, that means the neuron was only recently excised (stop codon taken out). That neuron therefore will not be visible. The longer the wait period after injections, the more neurons are able to induce pSTAT3. Given the limitations that no specific antibodies against LRb exist, both methods (pSTAT3 and GFP reporter expression) are important to visualize LRb neurons in the brain. However, it needs to be cautioned that not all central sites show a substantial overlap of both signals. This is particularly true for sites that are less accessible to circulating leptin than the ARC, e.g. the mPOA.

A benefit to using pSTAT3 involves the previously mentioned concept of leptin resistance. When leptin resistance is activated, a steady increase in pSTAT3 is observed that is ironically indicative of low leptin receptor function. Therefore, the high pSTAT3 induction with increasing body weight indicates leptin resistance. In measuring the effects of leptin resistance, pSTAT3 is highly effective because a shading of signaling capacity is seen.

This study concludes based on the data presented, that the ARC is an ideal site that shows appropriate representation of leptin receptor neurons via leptin-induced pSTAT3. While the mPOA and VMH do play roles in leptin action as derived from previous studies, their low colocalization percentages suggest that the pSTAT3 induction here may not be indicative of all leptin receptor neuron function. Additionally, the study concludes that GFP offers a representation of LRb neurons similar, but not identical in these two areas. Early development may be a main cause for the induction of pSTAT3 signals that are no longer visible and thus is not an appropriate method of quantifying leptin receptor neurons. The two methods of identifying leptin receptor neurons provide quality results based on the context of information, and each have their strengths. Future research can utilize the

findings of this study to branch out in multiple directions. One path includes studying the mPOA as well as other areas of the brain that show leptin-induced pSTAT3, whose influence on energy expenditure via leptin receptor neuronal pathways remains unknown. Another area of interest may involve innovating methods that maximize leptin-induced pSTAT3 for identifying LRb neuron populations. A surplus of information still remains undiscovered about these pathways and their effect on leptin action. Further research can provide the answers researchers seek in solving problems of today's growing obesity epidemic.

Acknowledgements

A special thank you goes to Dr. Heike Münzberg who guided me in the completion of this study and was always present to address any questions and concerns. Thank you to Dr. Amanda Laque for allowing me to use her animals and tissue sections for this study. Another thanks goes to Drs. Kavon Rezai-Zadeh and Sango Yu for encouraging questions and entertaining discussions pertaining to the study.

References

1) *Ahima, R. (2008). Revisiting leptin's role in obesity and weight loss. The Journal of Clinical Investigation, 118(7), 2380-2383.*
2) *Ahima, R., Prabakaran, D., Mantzoros, C., Qu, D., Lowell, B., Maratos-Flier, E., & Flier, J. (1996). Role of leptin in the neuroendocrine response to fasting. Nature, 382, 250-252.*
3) *Balthasar, N., Coppari, R., McMinn, J., Liu, S., Lee, C., Tang, V., Kenny, C., & McGovern, R. (2004). Leptin receptor signaling in pomc neurons is required for normal body weight homeostasis. Cell, 42, 983–991.*
4) *Banks, A., Davis, S., Bates, S., & Myers, M. (2000). Activation of downstream signals by the long form of the leptin receptor. J. Biol. Chem., 275(19), 14563–14572.*
5) *Bates, S., Dundon, T., Seifert, M., Carlson, M., Maratos-Flier, E., & Myers, M. (2004). Lrb-stat3 signaling is required for the neuroendocrine regulation of energy expenditure by leptin. Diabetes, 53, 3067-3073.*
6) *Bates, S., Stearns, W., Dundon, T., Schubert, M., Tso, A., Wang, Y., Banks, A., & Lavery, H. (2003). Stat3 signalling is required for leptin regulation of energy balance but not reproduction. Nature, 421, 856-859.*
7) *Belgardt, B., & Bruning, J. (2010). Cns leptin and insulin action in the control of energy homeostasis. Annals of the New York Academy of Sciences, 1212, 97-113.*
8) *Bjorbaek, C., Elmquist, J., Frantz, J. D., Soelson, S., & Flier, J. (1998). Identification of socs-3 as a potential mediator of central leptin resistance. Molecular Cell, 1, 619–625.*
9) *Bjorbaek, C., Lavery, H., Bates, S., Olson, R., Davis, S., Flier, J., Myers, M., & , (2000). Socs3 mediates feedback inhibition of the leptin receptor via tyr985. J. Biol. Chem., 275(51), 40649–40657.*
10) *Bjornholm, M., Münzberg, H., Leshan, R., Villanueva, E., Bates, S., Louis, G., Jones, J., & Ishida-Takahashi, R. (2007). Mice lacking inhibitory leptin receptor signals are lean with normal endocrine function. The Journal of Clinical Investigation, 117(5), 1354-1360.*
11) *Block, J., DeSalvo, K., & Fisher, W. (2003). Are physicians equipped to address the obesity epidemic? knowledge and attitudes of internal medicine residents. Preventative Medicine, 36, 669–675.*
12) *Cone, R., Cowley, M., Butler, A., Fan, W., Marks, D., & Low, M. (2001). The arcuate nucleus as a conduit for diverse signals relevant to energy homeostasis. International Journal of Obesity, 25(5), S63–S67.*
13) *Coppari, R., Ichinose, M., Lee, C., Pullen, A., Kenny, C., McGovern, R., Tang, V., & Liu, S. (2005). The hypothalamic arcuate nucleus: A key site for mediating leptin's effects on glucose homeostasis and locomotor activity. Cell Metabolism, 1, 63-72.*
14) *Couturier, C., & Jockers, R. (2003). Activation of the leptin receptor by a ligand-induced conformational change of constitutive receptor dimers. J. Biol. Chem., 278(29), 26604–26611.*
15) *Dhillon, H., Zigman, J., Ye, C., Lee, C., McGovern, R., Tang, V., Kenny, C., & Christiansen, L. (2006). Leptin directly activates sf1 neurons in the vmh, and this action by leptin is required for normal body-weight homeostasis. Neuron, 49, 191–203.*
16) *Flier, J. (1998). What's in a name? in search of leptin's physiologic role. Journal of Clinical Endocrinology and Metabolism, 83(5), 1407-1413.*
17) *Gong, Y., Ishida Takahashi, R., Villanueva, E., Fingar, D., Münzberg, H., & Myers, M. (2007). The long form of the leptin receptor regulates stat5 and ribosomal protein s6 via alternative methods. J. Biol. Chem., 282(42), 31019–31027.*
18) *Hill, J., Williams, K., Ye, C., Balthasar, N., Coppari, R., Cowley, M., Cantley, L., & Lowell, B. (2008). Acute effects of leptin require pi3k signaling in hypothalamic proopiomelanocortin neurons in mice. The Journal of Clinical Investigation, 118(5), 1796-1805.*
19) *Howard, J., Cave, B., Oksanen, L., Tzameli, I., Bjorbaek, C., & Flier, J. (2004). Enhanced leptin sensitivity and attenuation of dietinduced obesity in mice with haploinsufficiency of socs3. Nature Medicine, 10(7), 734-738.*

20) *Huo, L., Münzberg, H., Nillni, E., & Bjorbaek, C. (2004). Role of signal transducer and activator of transcription 3 in regulation of hypothalamic trh gene epression by leptin. Endocrinology, 145(5), 2516–2523.*
21) *Kalra, S. (2008). Central leptin insufficiency syndrome: An interactive etiology for obesity, metabolic and neural diseases and for designing new therapeutic interventions. Peptides, 29, 127–138.*
22) *Mori, H., Hanada, R., Hanada, T., Aki, D., Mashima, R., Nishinakumara, H., Torisu, T., & Chien, K. (2004). Socs3 deficiency in the brain elevates leptin sensitivity and confers resistance to diet-induced obesity. Nature Medicine, 10(7), 739-743.*
23) *Morrison, C. (2008). Leptin resistance and the response to positive energy balance. Physiology & Behavior, 94, 660-663.*
24) *Morton, G., Blevins, J., Williams, D., Niswender, K., Gelling, R., Rhodes, C., Baskin, D., & Schwartz, M. (2005). Leptin action in the forebrain regulates the hindbrain response to satiety signals. The Journal of Clinical Investigation, 115(3), 703-710.*
25) *Morton, G., Cummings, D., Baskin, D., Barsh, G., & Schwartz, M. (2006). Central nervous system control of food intake and body weight. Nature, 443, 289-295.*
26) *Münzberg, H. (2008). Differential leptin access into the brain — a hierarchical organization of hypothalamic leptin target sites? Physiology & Behavior, 2008, 664–669.*
27) *Münzberg, H., Björnholm, M., Bates, S., & Myers, M. (2005). Leptin receptor action and mechanisms of leptin resistance. Cellular and Molecular Life Sciences, 62, 642–652.*
28) *Münzberg, H., Huo, L., Nillni, E., Hollenberg, A., & Bjorbaek, C. (2003). Role of signal transducer and activator of transcription 3 in regulation of hypothalamic proopiomelanocortin gene expression by leptin. Endocrinology, 144(5), 2121–2131.*
29) *Münzberg, H., Jobst, E., Bates, S., Jones, J., Villanueva, E., Leshan, R., Bjornholm, M., & Elmquist, J. (2007). Appropriate inhibition of orexigenic hypothalamic arcuate nucleus neurons independently of leptin receptor/stat3 signaling. The Journal of Neuroscience, 27(1), 69-74.*
30) *Münzberg, H., & Myers, M. (2005). Molecular and anatomical determinants of central leptin resistance. Nature Neuroscience, 8(5), 566-570.*
31) *Myers, M., Cowley, M., & Münzberg, H. (2008). Mechanisms of leptin action and leptin resistance. Annu. Rev. Physiol., 70, 537–556.*
32) *Myers, M., Münzberg, H., Leinninger, G., & Leshan, R. (2009). The geometry of leptin action in the brain: More complicated than a simple arc. Cell Metab., 9(2), 117–123.*
33) *Robertson, S., Leinninger, G., & Myers, M. (2008). Molecular and neural mediators of leptin action. Physiology & Behavior, 94, 637–642.*
34) *Story, M., Neumark-Stzainer, D., Sherwood, N., Holt, K., Sofka, D., Trowbridge, F., & Barlow, S. (2002). Management of child and adolescent obesity: Attitudes, barriers, skills, and training needs among health care professionals. Pediatrics, 110(1), 210-214.*
35) *Taga, T. (1997). Gp130 and the interleukin-6 family of cytokines. Annu. Rev. Immunol., 15, 797–819.*
36) *Taniguchi, T. (1995). Cytokine signaling through nonreceptor protein tyrosine kinases. Science, 268, 251.*
37) *Tartaglia, L., Dembski, M., Weng, X., Deng, N., Culpepper, J., Devos, R., Richards, G., & Campfield, A. (1995). Identification and expression cloning of a leptin receptor, ob-r. Cell, 83, 1263-1271.*
38) *Wimalawansa, S. (2013). Visceral adiposity and cardiometabolic risks: epidemic of abdominal obesity in north america. Research and Reports in Endocrine Disorders, 3, 17-30.*
39) *White, D., Kuropatwinski, K., Devos, R., Baumann, H., & Tartaglia, L. (1997). Cytoplasmic domain mutationanal analysis and evidence for receptor homo-oligomerization. J. Biol. Chem., 272, 4065-4071.*
40) *White, D., & Tartaglia, L. (1996). Leptin and ob-r: Body weight regulation by a cytokine receptor. Cytokine & Growth Factor Reviews, 7(4), 303-309.*
41) *Zhang, Y., Kerman, I., Laque, A., Nguyen, P., Faouzi, M., Louis, G., Jones, J., & Rhodes, C. (2011). Leptin-receptor-expressing neurons in the dorsomedial hypothalamus and median preoptic area regulate sympathetic brown adipose tissue circuits. The Journal of Neuroscience, 31(5), 1873–1884.*